CEBAF PROPOSAL COVER SHEET

This Proposal must be mailed to:

CEBAF
Scientific Director's Office
12000 Jefferson Avenue
Newport News, VA 23606

and received on or before OCTOBER 30, 1989

A. TITLE: ELASTIC ELECTRON ^3He-^4He SCATTERING AT LARGE MOMENTUM TRANSFERS

B. CONTACT PERSON: GERASSIMOS G. PETRATOS (UNIVERSITY OF ROCHESTER)

ADDRESS, PHONE AND BITNET:

SLAC, BIN 44
P.O. Box 4349
Stanford, CA 94309
Phone: (415) 926-4361
Bitnet: GGP AT SLACVM

C. THIS PROPOSAL IS BASED ON A PREVIOUSLY SUBMITTED LETTER OF INTENT

☐ YES
☒ NO

IF YES, TITLE OF PREVIOUSLY SUBMITTED LETTER OF INTENT

D. ATTACH A SEPARATE PAGE LISTING ALL COLLABORATION MEMBERS AND THEIR INSTITUTIONS

(CEBAF USE ONLY)

Letter Received 10-31-89

Log Number Assigned PR-89-021

By KES

contact: Petratos

October 29, 1989

CEBAF Proposal

ELASTIC ELECTRON ^{3}He–^{4}He SCATTERING AT LARGE MOMENTUM TRANSFERS

P. E. Bosted, S. E. Rock
American University, Washington, D.C. 20016

K. A. Aniol, M. B. Epstein, D. J. Margaziotis
California State University, Los Angeles, CA 90032

J. J. LeRose, J. Mougey, A. Saha
CEBAF, Newport News, VA 23606

G. G. Petratos
University of Rochester, Rochester, NY 14627

S. E. Kuhn, Z. E. Meziani
Stanford University, Stanford, CA 94305

Spokesperson: G. G. Petratos

ABSTRACT

We propose to measure elastic electron ^{3}He and ^{4}He scattering to the highest momentum transfers possible, limited by a cross section sensitivity of about 2×10^{-42} cm^2/sr/MeV. The measurements will extend our knowledge of the magnetic-form factor of ^{3}He and the charge form-factor of ^{4}He down by two orders in magnitude and out in Q^2 possibly by a factor of two. The required incident beam energies range from 0.43 to 4.0 GeV. The scattered electrons will be detected in the Hall A High Resolution Spectrometer. A high-pressure, high-power target system of gas ^{3}He and ^{4}He with 25 cm long cells will be used. Good missing mass resolution will provide a clear separation from inelastic processes. The results are expected to play an important role in the understanding of the few-body structure at short distances and its description in terms of mesonic currents and/or quark and gluon-exchanges. We request 53 days of data taking at a current of 100μA and 7 days of checkout at low current, in a continuous two-month period or two one-month periods for each isotope.

1. MOTIVATION

Much of our understanding about the nucleon-nucleon force has come from the study of the few nucleon systems. In particular elastic electron scattering from ^{3}He and ^{4}He has played an important role in testing nuclear wave functions and theories of meson-exchange currents (MEC). In addition, it offers unique opportunities to examine the influence of many-body forces. Measurements at large momentum transfers may eventually lead to a better understanding of the role of the underlying quark constituents in nuclear structure.

The form-factors of ^{3}He, ^{3}H and ^{4}He have been in the past the subject of intense experimental[1–9] and theoretical[10–33] investigations. Recent measurements[4],[5],[6],[9] have separated the charge and magnetic form-factors of both trinucleon systems up to ~30 fm^{-2}. The charge form-factor of ^{4}He has been also measured[2],[5] up to Q^2=45 fm^{-2}. Figures 1, 2 and 3 show the form-factor data of ^{3}He and ^{3}H. Figure 4 shows the charge form-factor data of ^{4}He.

It is evident that the impulse approximation (IA) alone cannot describe the data correctly. As can be seen in Figures 1 and 2 ,the predicted diffraction minimum of ^{3}He and ^{3}H is calculated to be at higher (lower) momentum transfers for the charge (magnetic) form-factors than the data. The amplitude of the calculated second diffraction maximum is calculated to be significantly lower (higher) for the charge (magnetic) form-factors. In the case of ^{4}He the diffraction minimum is calculated to be at higher values of momentum transfers and the second maximum of the charge form-factor is also grossly underestimated (see Figure 5).

As in the case of the deuteron, the experimental data can not be explained without the explicit introduction of non-nucleonic degrees of freedom. The inclusion of meson-exchange currents as well as effects of isobaric configurations (IC) provides a reasonable description of the ^{3}He and ^{3}H data as can be seen in the calculations of Strueve *et. al.*,[24],[31] shown in Figures 1 and 2. The calculations of Hadjimichael *et. al.*,[23],[29] which include in addition the effect of genuine three-body force effects, offer also a fair description of the data. Similar calculations have been performed by Risca[20] and by Maize and Kim.[25] The former work examines in detail the sensitivity of the wave function and the hadronic form-factors in the exchange current operators, meanwhile the latter work offers an extensive investigation on the role of the principle of current conservation.

In the case of ^{4}He the inclusion of meson-exchange currents brings the calculated[15] charge form-factor closer to the observed values, but still strongly underestimates the height of the second maximum. The addition of three-body force effects[22] removes some of the remaining discrepancy, as shown in Figure 5.

An important question is whether mesonic and nucleonic degrees of freedom are sufficient for a quantitative understanding of the three- and four-body systems at large momentum transfers, where the nucleonic substructure and dynamics are generally recognized to make an increasing contribution and probably dominate. In recent years, several attempts have been made to simultaneously incorporate the quark- and gluon-exchange mechanism at short-distance and the meson-exchange mechanism at long- and intermediate-distance.

Kisslinger *et. al.*[26] have developed a hybrid quark-hadron (HQH) model for ^{3}He, which incorporate both nucleonic-mesonic and quark degrees of freedom. The main parameter is the separation $r_o \sim 1$ fm between the internal quark cluster region of overlapping nucleons and the external hadronic region, where the nucleons have little overlap and solutions to the Faddeev equations are used. A similar approach based on multi-quark compound states treated with the relativistic harmonic oscillator quark model has been followed by Maize and Kim.[27] Both models are in reasonable agreement with the form-factor data but they have a large model dependence.

Similar ideas have been employed in the treatment of the charge form-factor of ^{4}He. Namiki *et. al.*[21] have followed a multi-quark approach based also on the relativistic harmonic oscillator quark model that works fairly well in the region of large momentum transfers, but fails as the conventional nucleon-meson theories do, to reproduce the lower Q^2 data (see Figure 6). This model describes fairly well the ^{3}He forward data as can be also seen in Figure 6. The same degree of success is obtained in the composite meson-nucleon and 6-9-12 multiquark superposition approach followed by the Dubna group[32] as shown in Figure 7.

The hybrid models are in general able to reproduce the existing data but are still in a phenomenological stage and with sufficient freedom in the choice of elementary parameters used. The hope is that the hybrid models could provide a basis for a quantitative description of the short distance (quark) structure of the three- and four-body systems as well as for the deuteron and a bridge for treating short-range phenomena with a more fundamental QCD prescription.

The objective of this proposal is to extend the measurements of the magnetic form-factor F_{mag} of ^{3}He and the charge form-factor F_{ch} of ^{4}He to the highest momentum transfers possible, with a cross section sensitivity limit of about 2×10^{-42} cm^2/sr, and to make a careful mapping of the first diffraction minimum of ^{3}He. The results will put severe constraints in the theoretical calculations for the first diffraction minimum of ^{3}He , will test the diverging theoretical predictions at large momentum transfers and may lead to a better understanding of mesonic and quark-gluon degrees in the three- and four-body systems.

2. THE EXPERIMENT

2.1. Overview

We propose to measure backward (forward) elastic electron ^{3}He (^{4}He) scattering to the highest possible Q^2, limited to a form-factor error of less than 40%, in $\sim$ a week of beam time. The experiment will be performed into the Hall A facility using the HRS electron spectrometer. The required beam energy will be from 0.43 to 4.0 GeV. The scattering angle for all the ^{3}He data will be 165°. At this angle the cross section is dominated by the magnetic form-factor (except around the Q^2 region of its diffraction minimum). The contributions from the charge form-factor will be subtracted using the forward angle data of previous experiments.[4],[5] The scattering angle for the forward ^{4}He scattering will range from 14° to 26°. A detailed kinematic list is given in Tables 1 and 2.

The use of HRS is dictated by two reasons: a) the two-body threshold breakup of ^{3}He is only 5.5 MeV away from the elastic peak, requiring good momentum resolution and b) the elastic cross sections at large Q^2 are expected to fall in the 10^{-42} cm^{2}MeV^{-1}sr^{-1} range, requiring a large solid angle. The spectrometer will be instrumented with a standard configuration of a drift chamber set, a Cerenkov counter, a shower counter and two scintillation hodoscopes.

To maximize the counting rate the experiment must use the longest possible target consistent with resolution requirements and the maximum beam current consistent with the limitations of the target cooling system. This proposal assumes a realistic beam current of 100μA (half the Accelerator design value) and the use of 25 cm long high-power, high-density ^{3}He and ^{4}He targets. The resulting luminosity is 3.2×10^{38} cm^{-2}sec^{-1} for the ^{3}He case and 3.1×10^{38} cm^{-2}sec^{-1} for the ^{4}He case.

2.2. TARGET

The experiment will require the cryogenic high-pressure Helium gas target system planned for CEBAF, currently under design.[34] The target cells will be 25 cm long, consistent with resolution requirements, power dissipation limitations due to beam heating and mechanical design considerations.[35] The cells will be of parallelepiped shape with 0.381 mm Al endcaps and side walls, pressurized to 70 atm. The conceptual target design is similar to the 50 atm Helium gas target system used in SLAC experiment E121.[36] The circulation of the Helium gas will be transversely to the beam direction at a flow of 1-1.5 m/sec. The predicted density change under these conditions will be limited to ~1%.[35]

To eliminate the quasielastic scattering background from the Al endcaps two Tungsten collimating slits will be mounted on the support frame of the target cell towards the spectrometer side. The slits will mask the spectrometer from the endcaps and at the same time will define the effective target length seen by the spectrometer.

2.3. Detection System

The detection system will consist of a) a drift chamber set for reconstruction of the kinematical coordinates of the scattered electron, b) a gas threshold Cerenkov counter and a lead glass shower counter for particle identification and c) two scintillation hodoscopes. The pair of the Cerenkov and shower counters is needed to reject pion background and knock on electrons (produced in the drift chambers, the Cerenkov active medium etc.) as well as the large flux of cosmic muons. The first hodoscope will be placed between the Cerenkov and shower counters and will be used for triggering and for tracking assisting. The second hodoscope will be placed downstream of the shower counter to veto cosmic muons.

To keep the candidate event rate at a minimum level, the trigger logic will require either a coincidence among the Cerenkov counter, the first hodoscope and a minimal shower energy, or a coincidence between the first hodoscope and a large shower signal. This logic will also eliminate most of the cosmic ray background. The tight correlation of the position and angular divergence of the scattered electron in the drift chambers will leave no room for misidentification of cosmic rays as events coming from the target. The shielding of the spectrometer hut is expected to suppress the room background to a negligible level.

2.4. Missing Mass Resolution—Monte Carlo

The expected missing mass resolution ΔW was calculated using both analytic formulas and a Monte Carlo simulation program. The calculations have shown that the proposed experiment will have ample resolution to separate elastic from inelastic scattering. The missing mass resolution for the forward ^{4}He scattering is dominated by multiple scattering effects in the gas target and the Al cell, and for the backward ^{3}He scattering is dominated by Landau straggling of the incident beam. Contributions from the beam energy spread and the spectrometer angular and momentum resolutions are negligible.

The reconstructed elastic missing mass peak from the Monte Carlo program, plotted versus the excitation energy ($=W - M_{He}$), is shown for the highest kinematics for both ^{3}He and ^{4}He scattering in Figure 8. The Monte Carlo program simulated elastic electron Helium scattering taking properly into account the effects of energy loss and multiple scattering. Ionization loss was simulated using a parametrization of the Landau distribution function. The radiative energy losses were simulated using an approximation of the radiation probability distribution of Mo and Tsai. The incident and scattered electron angles were corrected for multiple scattering in the target media by simulating the Williams Gaussian distribution function. The program simulated also the angular and momentum resolutions of the spectrometer as well as the phase space of the incident and scattered electrons. The Figure shows for both ^{3}He and ^{4}He cases a clear separation between the elastic peak and the inelastic breakup threshold.

2.5. Data Acquisition–Analysis

The data acquisition will require modules from the nuclear electronics pool of the laboratory, and the computer data acquisition system and associated software of Hall A. The computer will be used for both logging of events onto storage media and on-line analysis. The on-line analysis software will be developed by the collaboration. The off-line analysis will be performed at the home institutions, with a minimal need of the computing resources of CEBAF.

3. RUN PLAN-COUNTING RATES

The cross section for elastic electron scattering from the spin 1/2 ^{3}He nucleus is given in terms of the charge and magnetic form-factors $F_{ch}(Q^2)$ and $F_{mag}(Q^2)$ by:

$$\frac{d\sigma}{d\Omega} = \sigma_M \left[A(Q^2) + B(Q^2)\tan^2\left(\frac{\theta}{2}\right)\right] \tag{3.1}$$

where σ_M is the Mott cross section and $A(Q^2)$ and $B(Q^2)$ are the elastic structure functions:

$$A(Q^2) = \frac{F_{ch}^2 + \mu^2\tau F_{mag}^2}{1+\tau} \tag{3.2}$$

$$B(Q^2) = 2\tau\mu^2 F_{mag}^2 \tag{3.3}$$

where $\tau = Q^2/4M_t^2$ and μ and M_t are the magnetic moment and mass of the target nucleus.

The cross section for elastic electron scattering from the spin 0 ^{4}He nucleus is given in terms of the charge form-factor $F_{ch}(Q^2)$ by:

$$\frac{d\sigma}{d\Omega} = \sigma_M \frac{F_{ch}^2(Q^2)}{1+\tau} \tag{3.4}$$

The expected cross sections for the backward ^{3}He scattering have been estimated using the existing data and the theoretical calculations of the full model of Hadjimichael *et. al.*.[23] The counting rates for the ^{4}He forward scattering are based on a linear extrapolation of the data of SLAC experiment E121.[5] The calculated rates are given in Tables 1 and 2 assuming 100μA beam current, 25 cm long, 70 atm gas targets, a solid angle of 8 msr and a radiative correction factor of 0.7. It can be seen that measurements up to $Q^2 \sim 55$ fm^{-2} for the ^{3}He magnetic form-factor and up to $Q^2 \sim 75$ fm^{-2} for the ^{4}He charge form-factor are possible at CEBAF. The new data will extend our form-factor knowledge down by two orders in magnitude. Depending on the actual on-line measured values of the form-factors, the allocation of running time to the different kinematical settings may vary, within the given beam time, using a sensitivity limit of a minimum of about ±40% form-factor error per kinematic point per week of running time. Tables 1 and 2 give also a possible allocation of beam time for the proposed kinematics. The Q^2 range and the quality of the possible form-factor data from this experiment are shown in Figures 9 and 10 along with the existing world data.

In addition to the elastic measurements the experiment requires a fair amount of checkout time to plateau all the counters, time the electronics and debug the on-line software. We estimate that about 7 days will be needed for the checkout process. The total requested time to perform the measurements can be either a continuous two month period or two separate one-month periods of beam time for each one of the two Helium isotopes.

4. SUMMARY

This experiment proposes to perform elastic electron Helium scattering to measure a) the magnetic form-factor of ^{3}He around the first diffraction minimum and at large momentum transfers, and b) the charge form-factor of ^{4}He at large momentum transfers. In summary we request use of a) the Hall A facilities with the HRS spectrometer instrumented for electron identification, b) a high-pressure, high-power gas Helium target system, c) the Hall A data acquisition system and d) 53 days of beam time for data taking and 7 days for checkout and calibrations. The experiment will produce data of fundamental importance to the understanding and advancement of modern nuclear physics.

REFERENCES

1. H. Collard *et. al.*, Phys. Rev. **138**, B57 (1965).
2. R. F. Frosch *et. al.*, Phys. Rev. **160**, 874 (1967).
3. M. Bernheim *et. al.*, Lett. Nuovo Cimento **5**, 431 (1972).
4. J. S. McCarthy *et. al.*, Phys. Rev. **C15**, 1396 (1977).
5. R. G. Arnold *et. al.*, Phys. Rev. Lett. **40**, 1429 (1978).
6. J. M. Cavedon *et. al.*, Phys. Rev. Lett. **49**, 987 (1982).
7. P. C. Dunn *et. al.*, Phys. Rev. **C27**, 71 (1983).
8. D. H. Beck *et. al.*, Phys. Rev. **C30**, 1403 (1984).
9. F-P. Juster *et. al.*, Phys. Rev. Lett. **55**, 2261 (1985).
10. E. P. Harper *et. al.*, Phys. Rev. Lett. **28**, 1533 (1972).
11. A. Laverne and C. Gignoux, Nucl. Phys. **A203**, 597 (1973).
12. M. R. Strayer and P. U. Sauer, Nucl. Phys. **A231**, 1 (1974).
13. R. A. Brandenburg *et. al.*, Phys. Rec. **C12**, 1368 (1975).
14. A. Barroso and E. Hadjimichael, Nucl. Phys. **A238**, 422 (1975).
15. J. Borysowicz and D. O. Risca, Nucl. Phys. **A254**, 301 (1975).
16. M. Gari *et. al.*, Nucl. Phys. **A271**, 365 (1976).
17. S. J. Brodsky and B. T. Chertok, Phys. Rev. **D14**, 3003 (1976).
18. I. A. Schmidt and R. Blankenbecler, Phys. Rev. **D15**, 3321 (1977).
19. B. T. Chertok, Phys. Rev. Lett. **41**, 1155 (1978).
20. D. O. Risca, Nucl. Phys. **350**, 227 (1980).
21. M. Namiki *et. al.*, Phys. Rev. **C25**, 2157 (1982).
22. T. Katayama *et. al.*, Prog. Theor. Phys. **67**, 236 (1982).

23. E. Hadjimichael *et. al.*, Phys. Rev. **C27**, 831 (1983).

24. W. Strueve *et. al.*, Nucl. Phys. **A405**, 620 (1983).

25. M. A. Maize and Y. E. Kim, Nucl. Phys. **A420**, 365 (1984).

26. J. L. Friar *et. al.*, Ann. Rev. Nucl. Part. Sci. **34**, 403 (1984).

27. M. A. Maize and Y. E. Kim, Phys. Rev. **C31**, 1923 (1985).

28. L. S. Kisslinger *et. al.*, Nucl. Phys. **A459**, 645 (1986).

29. E. Hadjimichael, Phys. Lett. **B172**, 156 (1986).

30. J. M. Lina and B. Goulard, Phys. Rev. **C34**, 714 (1986).

31. W. Strueve *et. al.*, Nucl. Phys. **A465**, 651 (1987).

32. V. V. Burov and V. K. Lukyanov, Nucl. Phys. **A463**, 263c (1987).

33. H. Dijk and M. Beyer, Paul Scherrer Institut Preprint PSI-PR-89-20 (1989).

34. D. J. Margaziotis, private communication.

35. J. W. Mark, private communication.

36. D. B. Day, Ph.D. Thesis, University of Virginia (1979).

TABLE CAPTIONS

1: The kinematics of the proposed experiment for backward elastic scattering from ^{3}He. The electron scattering angle is fixed at 165°. Also given is a possible run plan, cross section estimates and counting rates. The cross sections use the full model values of F_{mag} by Hadjimichael *et. al.*[23] and the large momentum transfer forward data from SLAC experiment E121.[5] The rate estimates assume a 25 cm, 70 atm ^{3}He gas target, 100 μA beam current, 8 msr spectrometer solid angle and a radiative correction factor of 0.7.

2: The kinematics of the proposed experiment for forward elastic scattering from ^{4}He. The incident beam energy is fixed at 4 GeV. Also given is a possible run plan, cross section estimates and counting rates. The cross sections assumed are a linear extrapolation of the large momentum transfer forward data from SLAC experiment E121.[5] The rate estimates assume a 25 cm, 70 atm ^{4}He gas target, 100 μA beam current, 8 msr spectrometer solid angle and a radiative correction factor of 0.7.

TABLE 1

^{3}He RUN PLAN - RATES

$\theta = 165°$

Target = 25 cm ^{3}He

Density = 0.098 g/cm^3

Current = 100 μA

$\Delta\Omega$ = 8 msr

Rad. Cor. factor = 0.7

Q^2 (fm^{-2})	E (GeV)	E' (GeV)	Cross Section (nb/sr/GeV)	Time (h)	Counts F_{ch}	Counts F_{mag}	ΔF_{mag} (±%)
14.1	0.43	0.33	8.6E−05	1	151	381	8
18.1	0.49	0.36	4.0E−05	40	7001	2796	35
20.2	0.52	0.38	4.3E−05	3	282	516	11
22.6	0.56	0.40	3.5E−05	2	98	340	8
25.0	0.59	0.42	2.9E−05	2	50	312	6
30.3	0.66	0.45	1.2E−05	2	12	136	6
36.0	0.73	0.49	3.5E−06	4	5	81	7
42.3	0.81	0.52	7.7E−07	7	2	32	11
50.0	0.89	0.55	5.8E−08	52	3	16	16
56.3	0.97	0.58	6.2E−09	252	2	7	38
TOTAL				365			
TOTAL		60%	Efficiency	608			

TABLE 2

^{4}He RUN PLAN - RATES

$E = 4$ GeV

Target = 25 cm ^{3}He

Density = 0.136 g/cm^3

Current = 100 μA

$\Delta\Omega = 8$ msr

Rad. Cor. factor = 0.7

Q^2 (fm^{-2})	θ (deg.)	E' (GeV)	Cross Section (nb/sr/GeV)	Time (h)	Counts	ΔF_{ch} ($\pm$%)
25	14.4	3.87	3.5E−02	1	226000	0.1
30	15.8	3.84	5.7E−03	1	37000	0.3
35	17.2	3.82	9.9E−04	1	6390	0.6
40	18.4	3.79	1.8E−04	1	805	1.5
45	19.6	3.76	3.3E−05	2	365	2.4
50	20.8	3.74	6.3E−06	4	158	3.9
55	21.9	3.71	1.2E−06	9	71	5.8
60	23.0	3.69	2.4E−07	19	30	8.7
65	24.0	3.66	4.8E−08	44	14	12.6
70	25.0	3.63	9.8E−09	97	6	18.7
75	26.0	3.61	2.0E−09	210	3	25.6
TOTAL				389		
TOTAL		60%	Efficiency	648		

FIGURE CAPTIONS

1) The charge form-factors of ^{3}He and ^{3}H. The dashed curve is the impulse approximation. The solid curve includes in addition π- and ρ-mesonic currents as well as contributions from isobaric configurations.[31]

2) The magnetic form-factors of ^{3}He and ^{3}H. The dashed curve is the impulse approximation. The solid curve includes in addition π- and ρ-mesonic currents as well as contributions from isobaric configurations.[31]

3) The ^{3}He elastic structure function $A(Q^2)$ (see Chapter 3) data from Stanford, Orsay and SLAC compared to theoretical calculations. The solid curve is calculated from the Faddeev wave function in momentum space[13]; the dotted curve (indistinguishable from the solid one up to $\sim$57 fm^{-2}) is a similar calculation in configuration space[11]; the dot-dashed curve includes meson-exchange currents from Ref. 15; the small-dashed curve is the calculation of the dimensional scaling quark model[17] and the long-dashed is a relativistic impulse approximation calculation.[18]

4) The charge form-factor data of ^{4}He from Stanford and SLAC compared to theoretical calculations. The solid curve is the impulse approximation of Ref. 15; the dotted curve includes MEC;[16] the small-dashed curve is the calculation of the dimensional scaling quark model[17] and the long-dashed is a relativistic impulse approximation calculation.[18]

5) Effects of meson-exchange currents on the ^{4}He charge form-factor for a) the Hamada-Johnston potential and b) with the inclusion of a three-body force potential. In b) the three-body effect on the impulse approximation is also shown by the dotted line.[22]

6) The calculation of the relativistic harmonic oscillator quark model of Namiki *et. al.*[21] (solid line), compared to the experimental data for: a) the elastic structure function $A(Q^2)$ of ^{3}He and b) the charge form-factor of ^{4}He . In a) the dotted line is the ordinary nuclear theory calculation of Ref. 13 , and in

b) is the conventional meson-nucleon model calculation of Ref. 22.

7) The charge form-factor of ^{4}He from the composite meson-nucleon multi-quark superposition model of Ref. 32 (solid curve) compared to the experimental data. The calculation includes, in addition to the impulse approximation (shown as the dotted line), meson-exchange currents and terms from 6-quark, 9-quark and 12-quark admixtures in the nuclear wave function.

8) The reconstructed elastic peak from the Monte Carlo simulation program of the proposed experiment, plotted versus the excitation energy ($=W - M_{He}$), for the highest extreme kinematics: a) elastic electron ^{3}He scattering with a 25 cm long, 2.5 g/cm^2 thick ^{3}He target at a scattering angle of 165° and a beam energy of 1.0 GeV (Q^2= 55 fm^{-2}); b) elastic electron ^{4}He scattering with a 25 cm long, 3.4 g/cm^2 thick ^{4}He target at a beam energy of 4.0 GeV and a scattering angle of 26° (Q^2= 75 fm^{-2}).

9) Possible data on the magnetic form-factor of ^{3}He from this experiment, based on the model by Hadjimichael.[23] Also shown are the Stanford[4] and Saclay[6] data.

10) Possible data on the charge form-factor of ^{4}He from this experiment, based on a linear extrapolation of the existing data. Also shown are the Stanford[2] and SLAC[5] data.

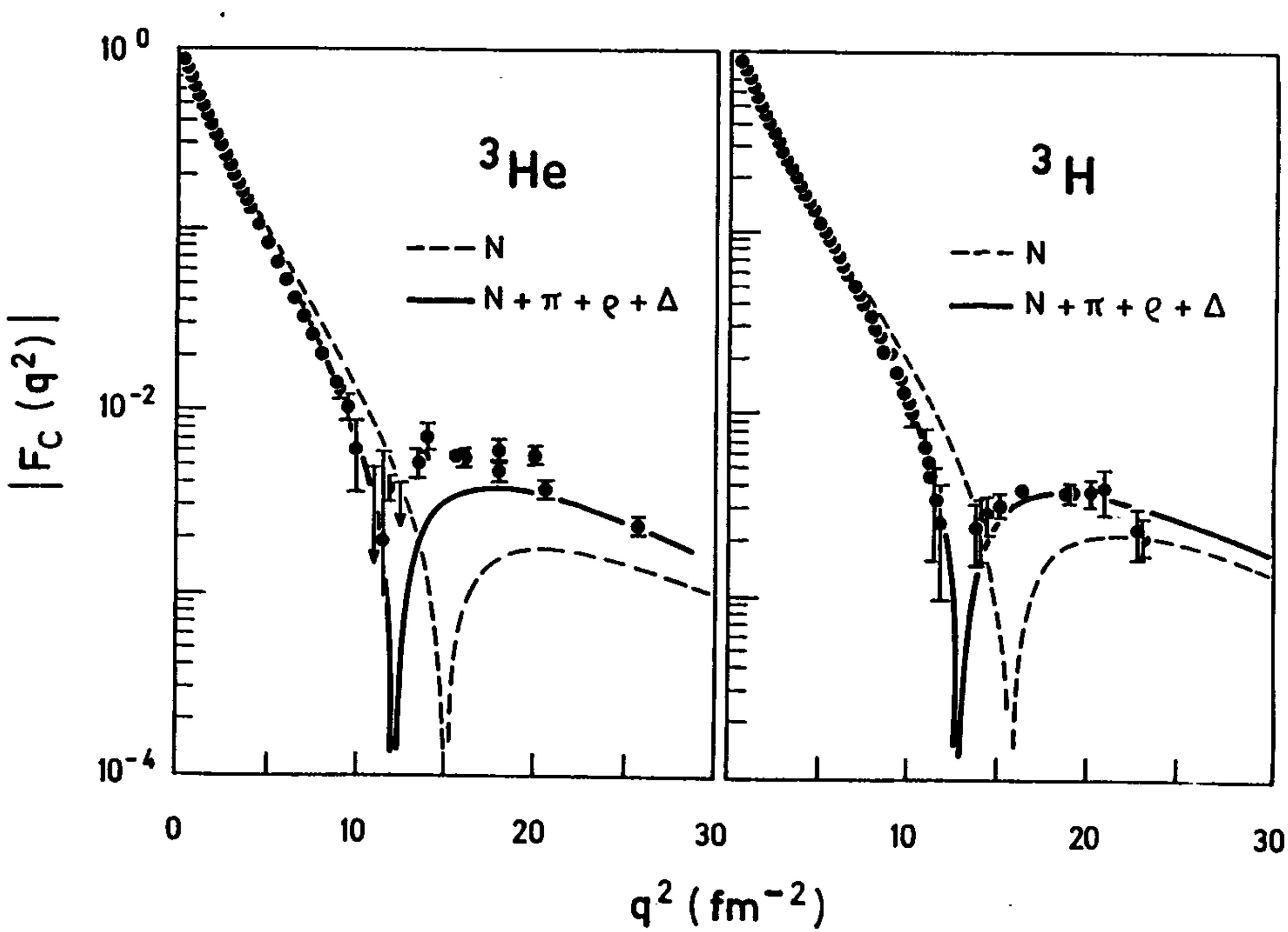

Figure 1

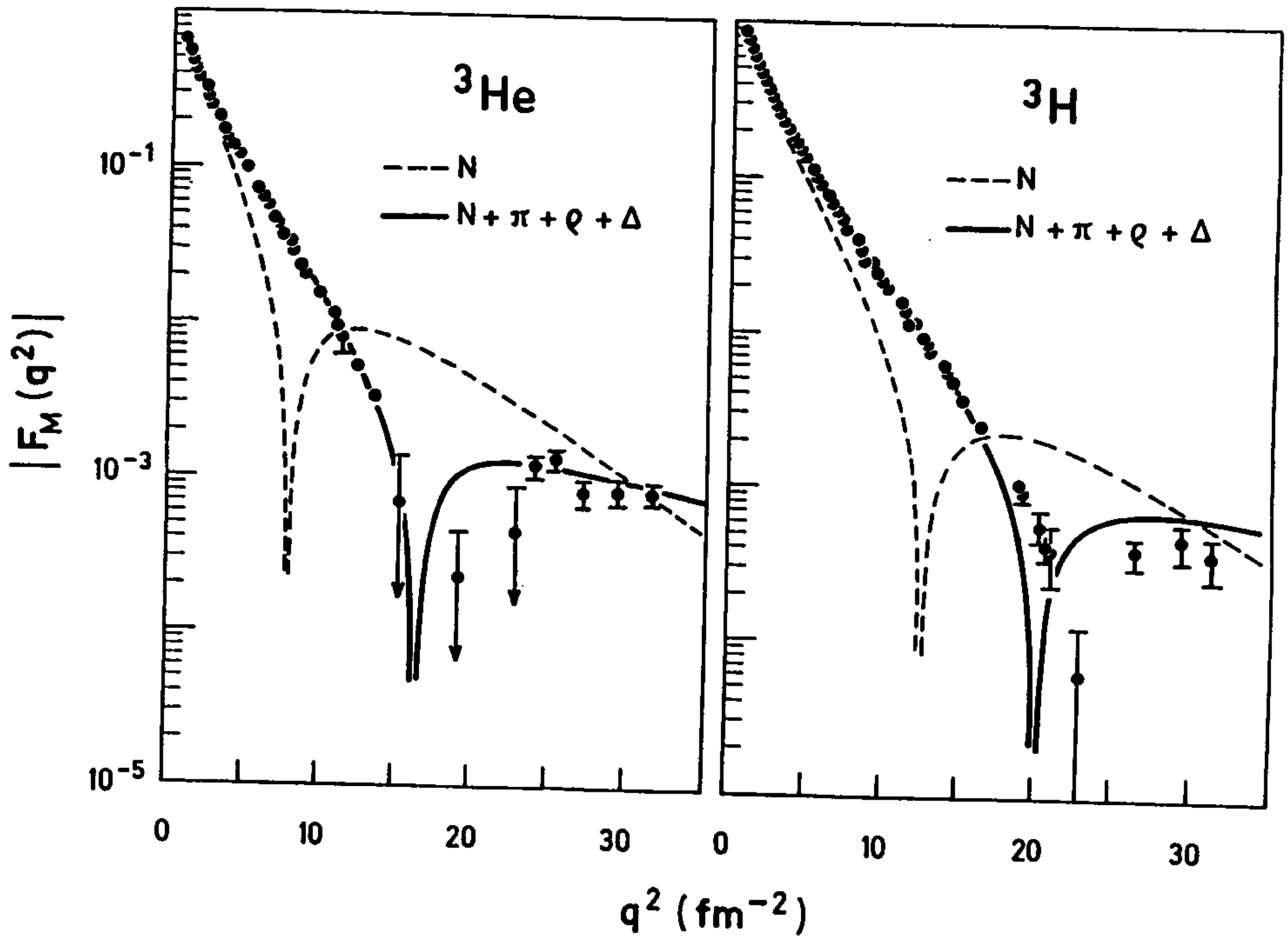

Figure 2

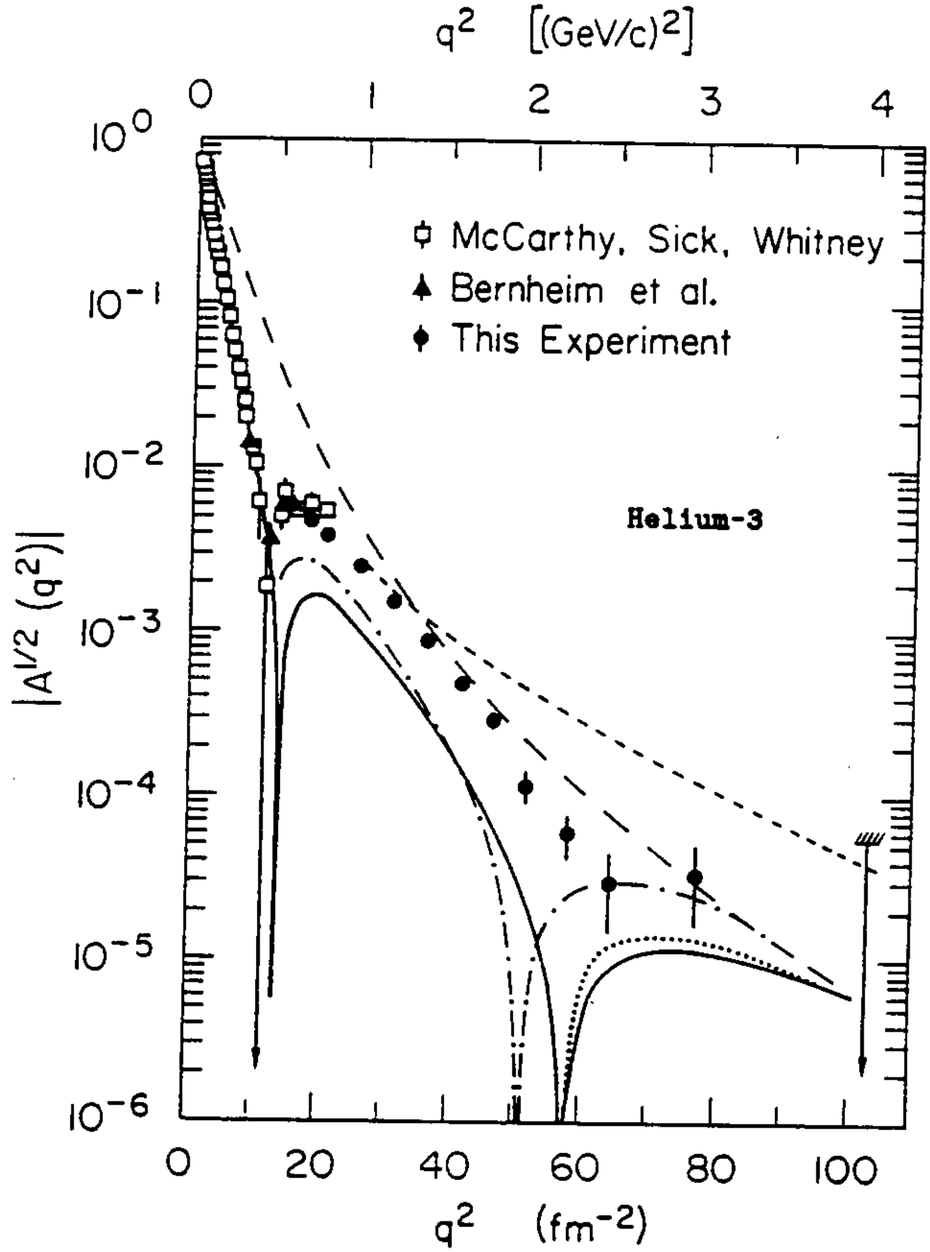

q2 [(GeV/c)2]
0
1
2
3
4
10^0
10^-1
10^-2
10^-3
10^-4
10^-5
10^-6
McCarthy, Sick, Whitney
Bernheim et al.
This Experiment
Helium-3
|A1/2 (q2)|
0
20
40
60
80
100
q2 (fm-2)

Figure 3

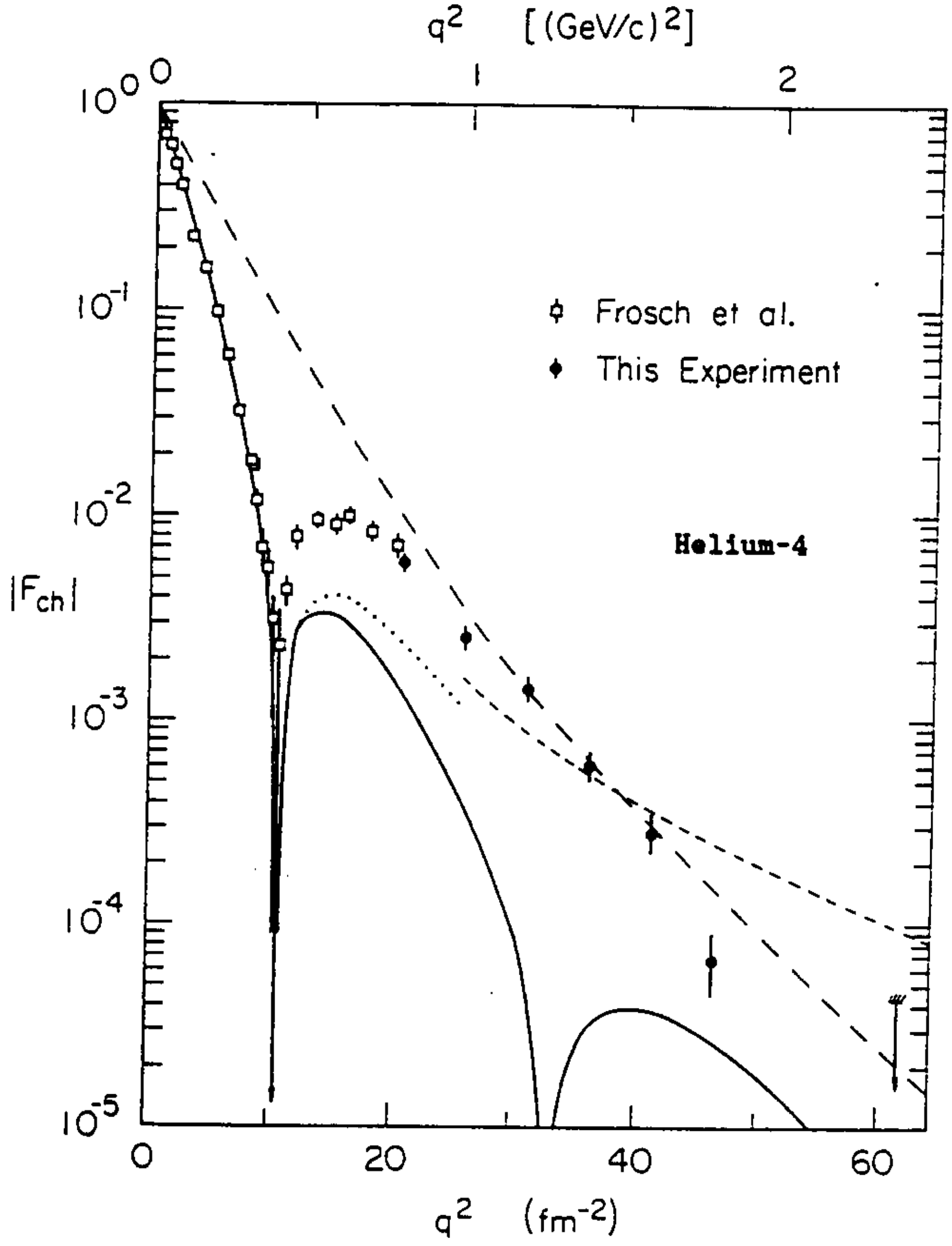
q^2 [(GeV/c)^2]
0
1
2
10^0
10^{-1}
10^{-2}
10^{-3}
10^{-4}
10^{-5}
$|F_{ch}|$
Frosch et al.
This Experiment
Helium-4
0
20
40
60
q^2 (fm^{-2})

Figure 4

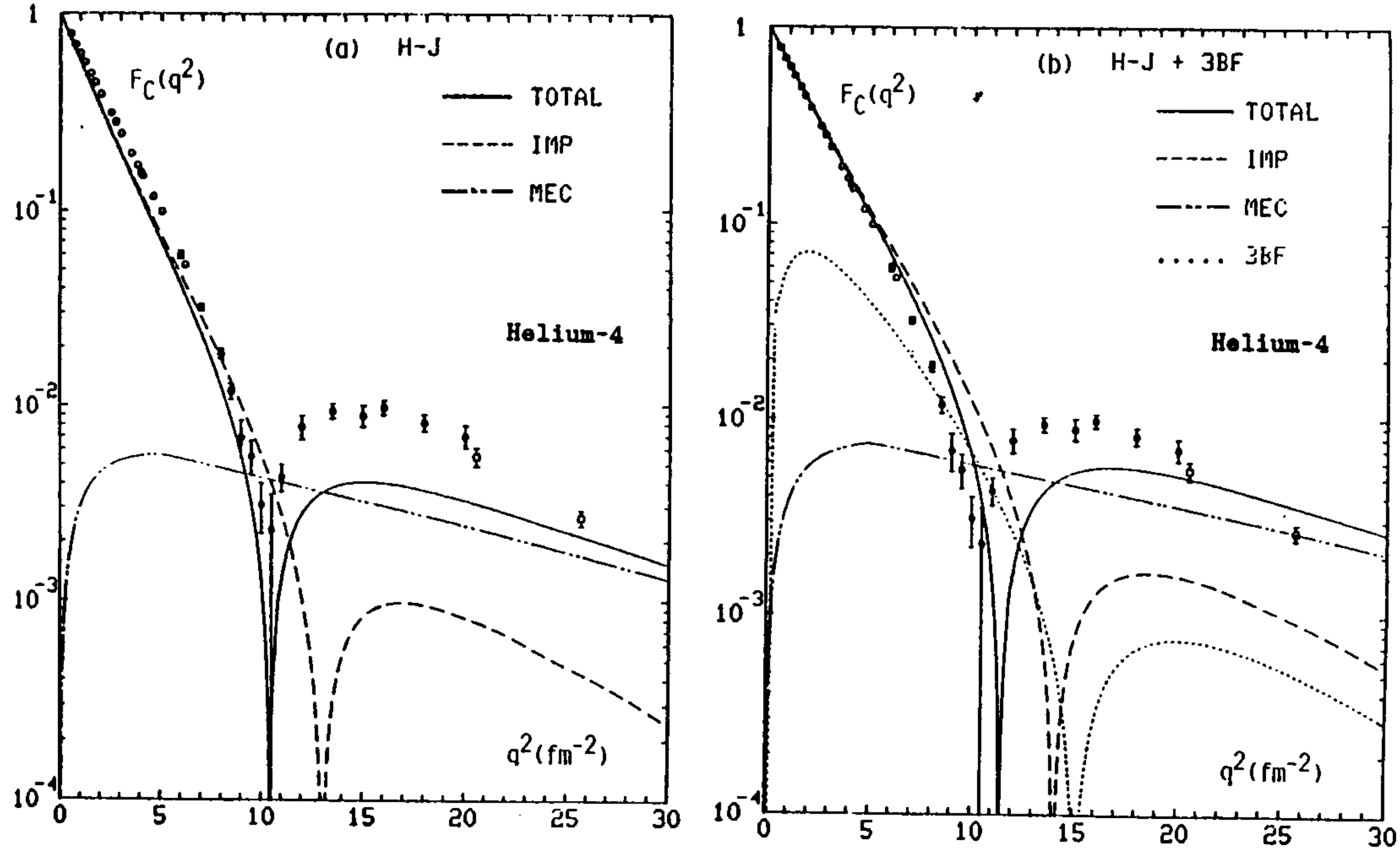

(a) H-J
$F_C(q^2)$
TOTAL
IMP
MEC
Helium-4
$q^2(fm^{-2})$
(b) H-J + 3BF
$F_C(q^2)$
TOTAL
IMP
MEC
3BF
Helium-4
$q^2(fm^{-2})$

Figure 5

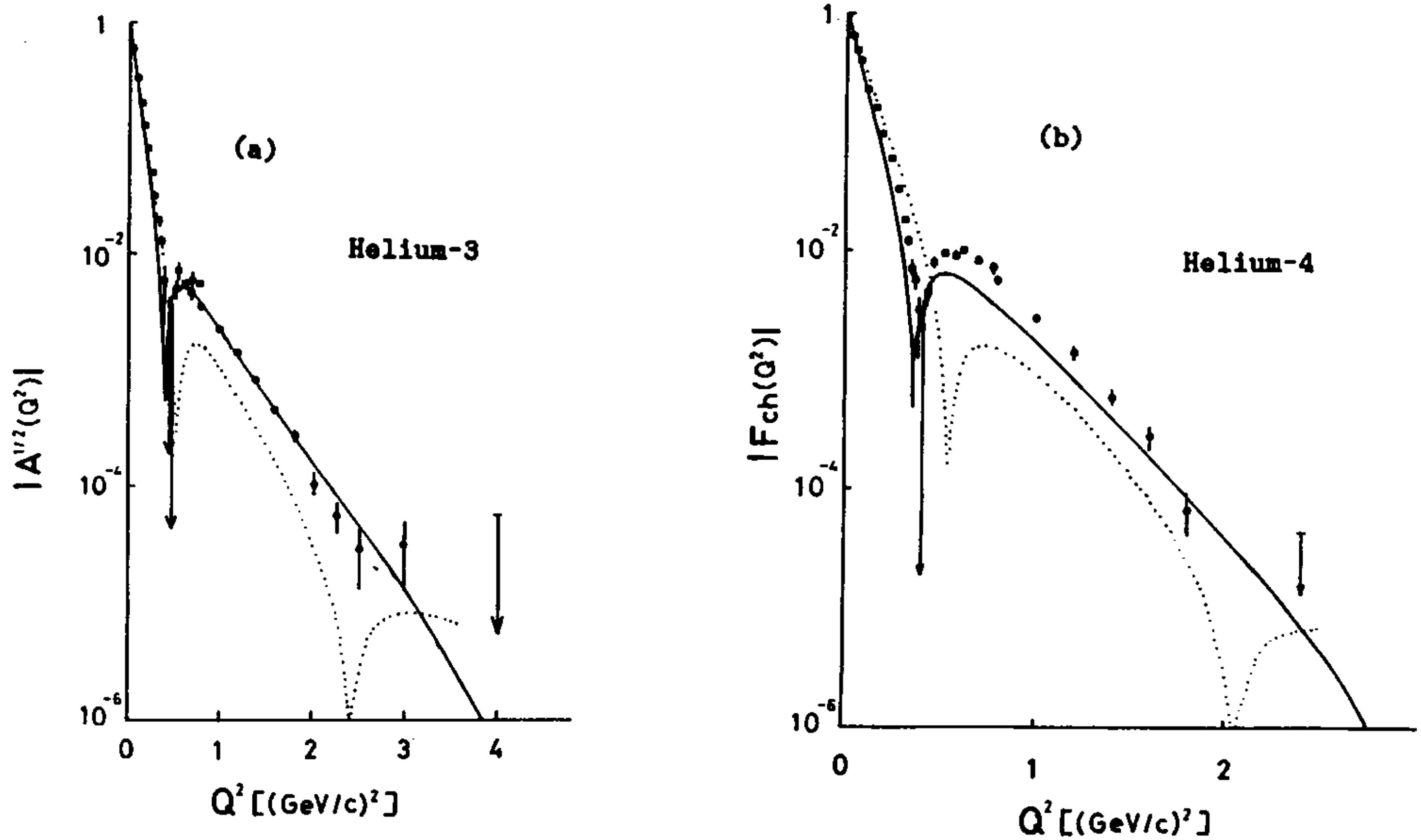

(a)
Helium-3
|A^{1/2}(Q^2)|
1
10^-2
10^-4
10^-6
0
1
2
3
4
Q^2 [(GeV/c)^2]
(b)
Helium-4
|F_ch(Q^2)|
1
10^-2
10^-4
10^-6
0
1
2
Q^2 [(GeV/c)^2]

Figure 6

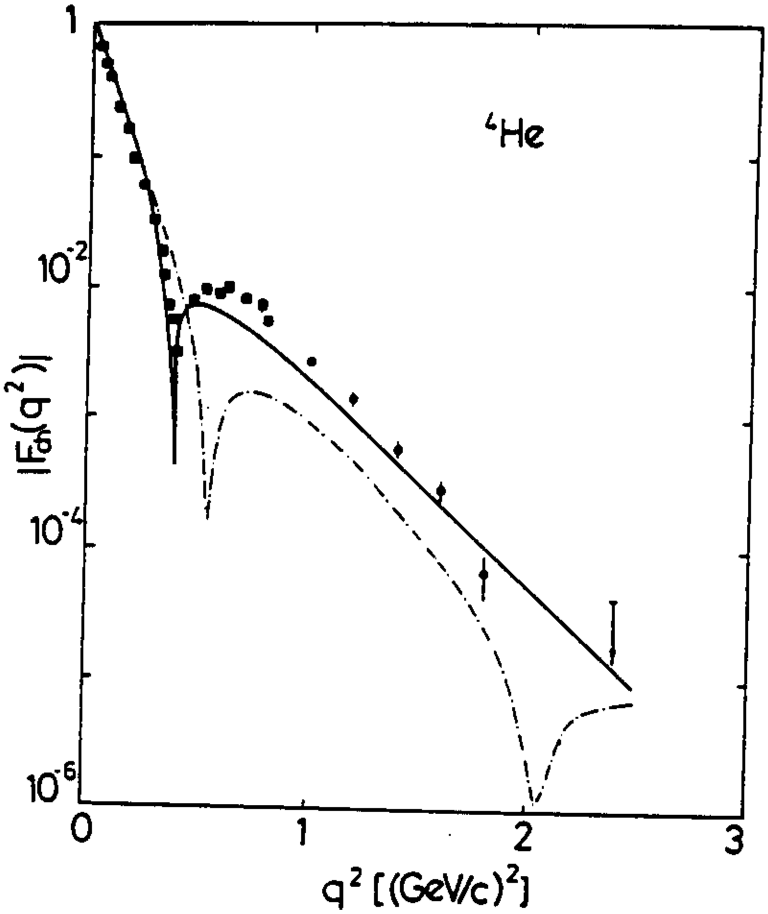

Figure 7

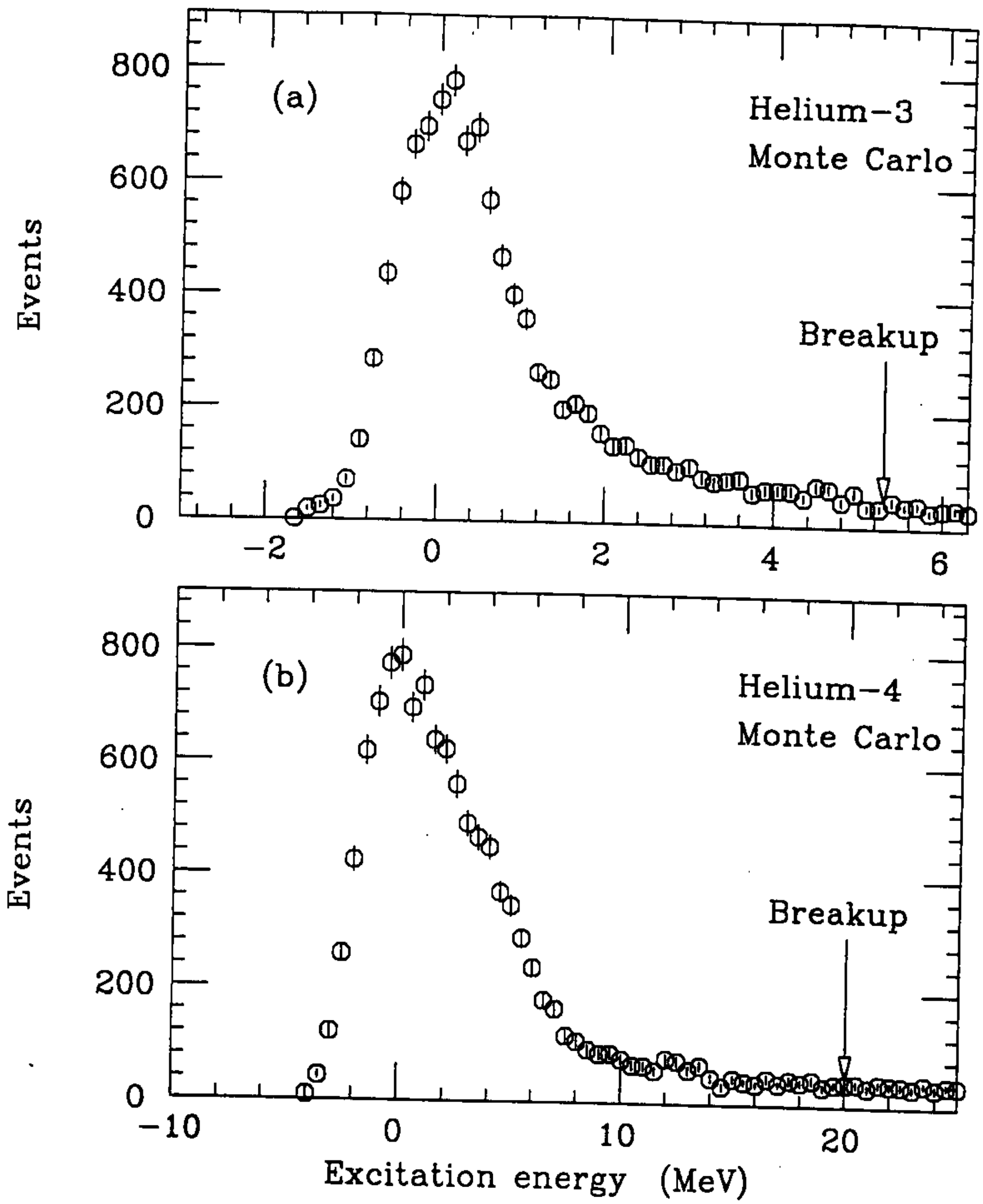

(a)
Helium−3
Monte Carlo
Breakup
Events
800
600
400
200
0
−2
0
2
4
6
(b)
Helium−4
Monte Carlo
Breakup
Events
800
600
400
200
0
−10
0
10
20
Excitation energy (MeV)

Figure 8

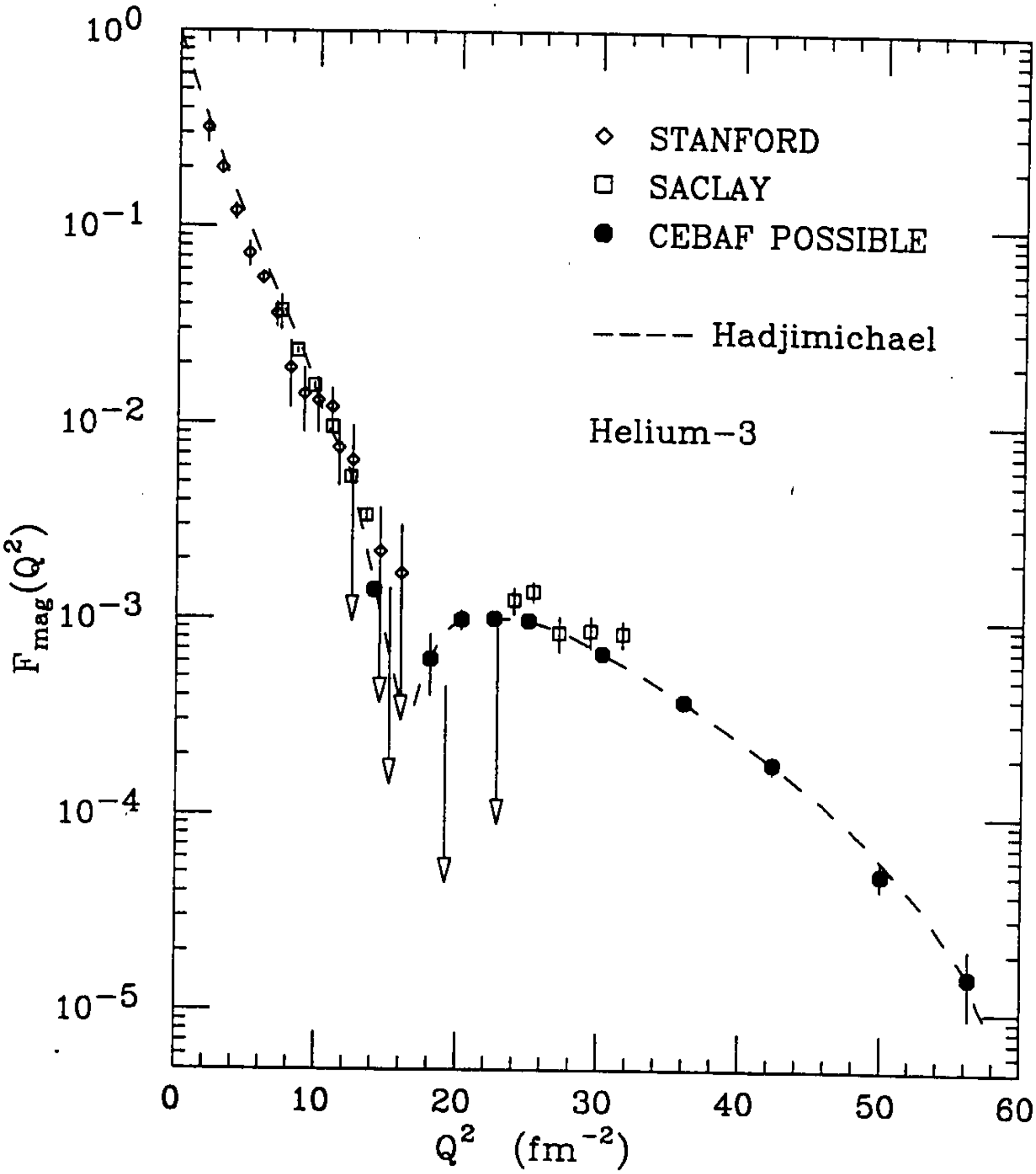
STANFORD
SACLAY
CEBAF POSSIBLE
Hadjimichael
Helium-3
$F_{mag}(Q^2)$
Q^2 (fm^{-2})
10^0
10^{-1}
10^{-2}
10^{-3}
10^{-4}
10^{-5}
0
10
20
30
40
50
60

Figure 9

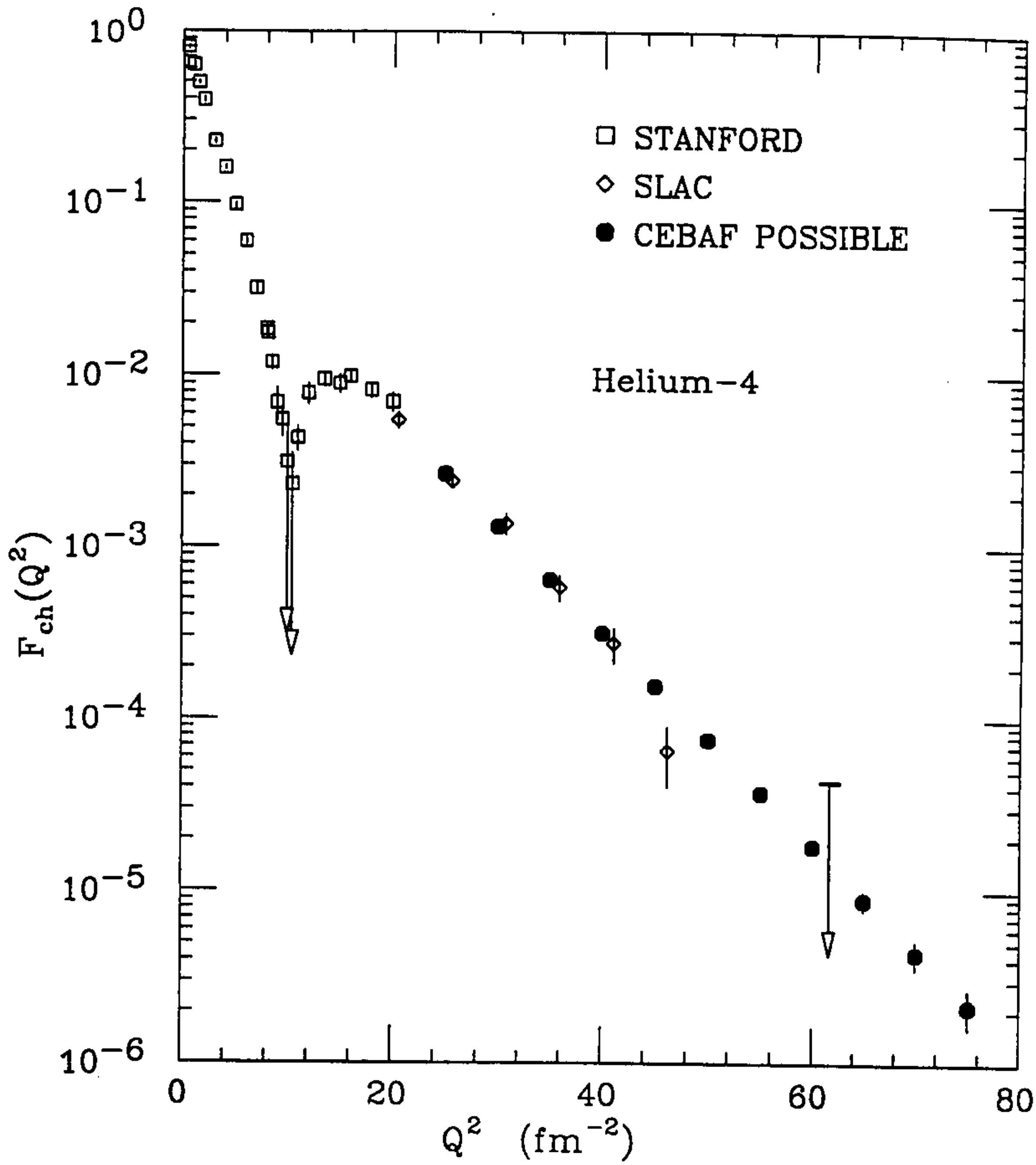

STANFORD
SLAC
CEBAF POSSIBLE
Helium-4
10^{0}
10^{-1}
10^{-2}
10^{-3}
10^{-4}
10^{-5}
10^{-6}
$F_{ch}(Q^2)$
0
20
40
60
80
Q^2 (fm^{-2})

Figure 10

March 1990

ADDENDUM
PROPOSAL CEBAF-PR-89-21 (G. G. Petratos *et. al.*)

ELASTIC ELECTRON ^{3}He–^{4}He SCATTERING AT LARGE MOMENTUM TRANSFERS

This appendix gives a comparison between the elastic electron-^{3}He experiment proposed at CEBAF and the recently submitted and approved elastic electron-^{3}He MIT-Bates experiment. Though the kinematical and luminosity capabilities of CEBAF are unsurpassed by any of the existing electron machines, this addendum/comparison is necessary as the Bates proposal was submitted after the submission and presentation of the CEBAF proposal.

The CEBAF experiment will use the electron High Resolution Spectrometer (HRS) of Hall-A to measure both backward and forward scattering. The backward scattering will use the HRS in its large solid angle mode (15 msr) at 158° and a cryogenic high-pressure ^{3}He target. The proposal assumes use of a 20 K, 70 atm, 17 cm long target resulting in a thickness of 1.70 g/cm^2. Note that the Hall-A Conceptual Design Report calls for the construction of a higher density (10 K, 70 atm) target system.[2] The forward scattering will use HRS in its standard solid angle mode (8 msr) and a target 0.85 g/cm^2 thick. The proposal also assumes a beam intensity of 100 μA (half the accelerator design value). The luminosity of the backward scattering is 3.2 $\times 10^{39}$ cm^{-2}sec^{-1}msr.

The Bates experiment will use the Energy Loss Spectrometer System (ELSSY) of North Hall with a solid angle of 3 msr at its maximum angle of 160°. The proposal calls for the construction of a 24 K, 50 atm, 7 cm long target resulting in a density of 0.53 g/cm^2. The experiment will use an average current of 30 μA. The above factors will provide a luminosity of 5.8 $\times 10^{37}$ cm^{-2}sec^{-1}msr. The data analysis will use the forward angle data on the $A(Q^2)$ elastic structure function from SLAC experiment E121[3] to separate the magnetic and charge form-factors.

A summary of the kinematical and luminosity parameters of the two experiments is given in Table 1. The important differences between the two experiments are in luminosity and the maximum momentum transfer attainable. The luminosity of the CEBAF experiment is *55 times larger* than that of the Bates experiment. The maximum Q^2 at Bates will be 54.3 fm^{-2}, *limited by the accelerator beam energy.* At CEBAF, the maximum Q^2 will be limited by the cross section fall-off rather than the machine energy limit, which is 420 fm^{-2} (for the backward scattering).

A comparison in the sensitivity limit of the two experiments is given in Figures 1 and 2. The Figures also show the predictions of the calculations of three theoretical groups: Schiavilla *et. al.*,[4] Strueve *et. al.*,[5] and Hadjimichael *et. al.*[6] For the F_{mag} magnetic form-factor, the sensitivity limit is defined as the lowest value that can be measured with ±30% statistical error. This corresponds to a bacward elastic count rate of 0.6/day and a realistic low limit of 3 events in 5 days of running (±60% statistical cross section error) with 100% efficiency. The Bates proponents plan of spending a maximum of 5 days of running (at 100% efficiency) at the highest Q^2 setting.

In the CEBAF case, the charge form-factor will be separated by measuring also forward scattering. Figure 2 shows the lowest value of F_{ch} that can be measured at CEBAF assuming a) the backward limit of 3 counts in 5 days and b) an arbitrary low elastic event rate of 8/day at a forward angle of 30°. In 1 day of running with 100% efficiency the F_{ch} statistical error will be about ±30%. In the Bates case, the charge form-factor will be extracted using the $A(Q^2)$ SLAC data. The extracted F_{ch} value that corresponds to the above backward scattering limit is shown in Figure 2. The average error in the Q^2 range of the Bates proposal (30.2 to 54.3 fm^{-2}) will be also about ±30%.

Figures 1 and 2 clearly show that the CEBAF form-factor sensitivity is one order of magnitude lower than that of the Bates experiment. The Bates experiment can extend the form-factor measurements down to the 10^{-4} limit and only out to Q^2=54.3 fm^{-2}. The Bates sensitivity/kinematical limits will not allow a measurement of the second diffraction minimum and third maximum of the ^{3}He form-factors as predicted by all three theoretical calculations. The CEBAF experiment will clearly be capable of allowing these measurements, and in any case will extend our knowledge of both ^{3}He elastic form-factors down to the 10^{-5} level.

REFERENCES

1. MIT/Bates Proposal, *Measurement of the elastic magnetic form-factor of ^{3}He at high momentum transfer*, H. Baghaei, G. Peterson *et. al.*, Dec. 1989.
2. *CEBAF HALL-A Conceptual Design Report (CDR)*, in preparation; D. J. Margaziotis, private communication.
3. R. G. Arnold *et. al.*., Phys. Rev. Lett. **40**, 1429 (1978).
4. R. Schiavilla *et. al.*, Phys. Rev. **C41**, 309 (1990);
   R. Schiavilla and D. O.Riska, University of Helsinki preprint HU-TFT-90-15 (1990), submitted to Phys. Lett. B;
   R. Schiavilla, private communication.
5. W. Strueve *et. al.*, Nucl. Phys. **A465**, 651 (1987);
   C. Hadjuk, in *Proceedings of the 1984 CEBAF Summer Workshop*, Newport News, 1984, edited by F. Gross and R. Whitney.
6. E. Hadjimichael *et. al.*, Phys. Rev. **C27**, 831 1983.

TABLE 1

CEBAF - MIT/Bates Comparison

Backward Elastic ^{3}He Scattering

	Bates	CEBAF
Scattering angle	160°	158°
Maximum Q^2 (fm^{-2})	54.3	420
Solid angle (msr)	3.0	15.0
Target thickness (g/cm^2)	0.53	1.7
Beam current (μA)	30	100
Luminosity ($cm^{-2}sec^{-1}msr$)	5.8×10^{37}	3.2×10^{39}

FIGURE CAPTIONS

1) The sensitivity limit in the ^{3}He magnetic form-factor measurement at CEBAF and Bates compared with theoretical predictions. The sensitivity limit is defined as the lowest form-factor value that can be measured with a $\pm30\%$ statistical error. This corresponds to a backward count rate of 0.6/day and a realistic low limit of 3 elastic events in 5 days of running ($\pm60\%$ statistical cross section error) at 100% efficiency. a) Theoretical prediction of Schiavilla *et. al.* (Ref. 4) using four different nucleon form-factor sets (solid curve: GK, dashed curve: IJL, dotted curve: Hohler, dot-dashed curve: dipole), b) Theoretical prediction by Hadjimichael *et. al.* (Ref. 6), c) Theoretical prediction by Strueve *et. al.* (Ref. 5).

2) The sensitivity limit in the ^{3}He charge form-factor measurement compared with theoretical predictions. The CEBAF case sensitivity limit assumes a) the backward limit of 3 counts in 5 days and b) an arbitrary low elastic event rate of 8/day at a forward angle of 30°. In 1 day of running with 100% efficiency the F_{ch} statistical error will be about $\pm30\%$. In the Bates case the charge form-factor is calculated using a) the backward limit of 3 counts in 5 days and b) the measured $A(Q^2)$ SLAC data (Ref. 3). The average error in the Q^2 range of the Bates proposal (30.2 to 54.3 fm^{-2}) will be also about $\pm30\%$. a) Theoretical prediction of Schiavilla *et. al.* (Ref. 4) using four different nucleon form-factor sets (solid curve: GK, dashed curve: IJL, dotted curve: Hohler, dot-dashed curve: dipole), b) Theoretical prediction by Hadjimichael *et. al.* (Ref. 6), c) Theoretical prediction by Strueve *et. al.* (Ref. 5).

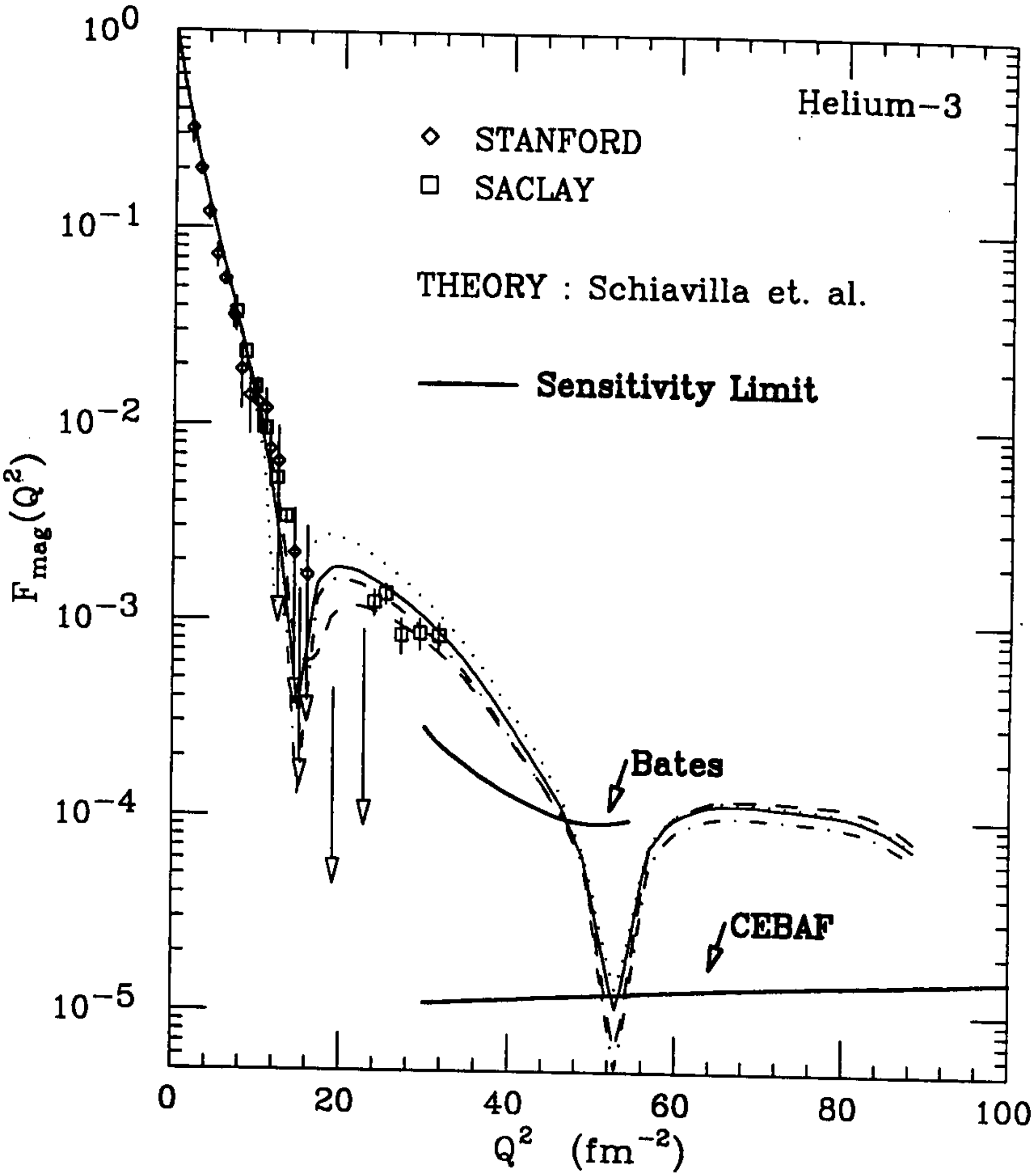

Helium−3
STANFORD
SACLAY
THEORY : Schiavilla et. al.
Sensitivity Limit
Bates
CEBAF
10^0
10^{-1}
10^{-2}
10^{-3}
10^{-4}
10^{-5}
0
20
40
60
80
100
$F_{mag}(Q^2)$
Q^2 (fm^{-2})

Figure 1a

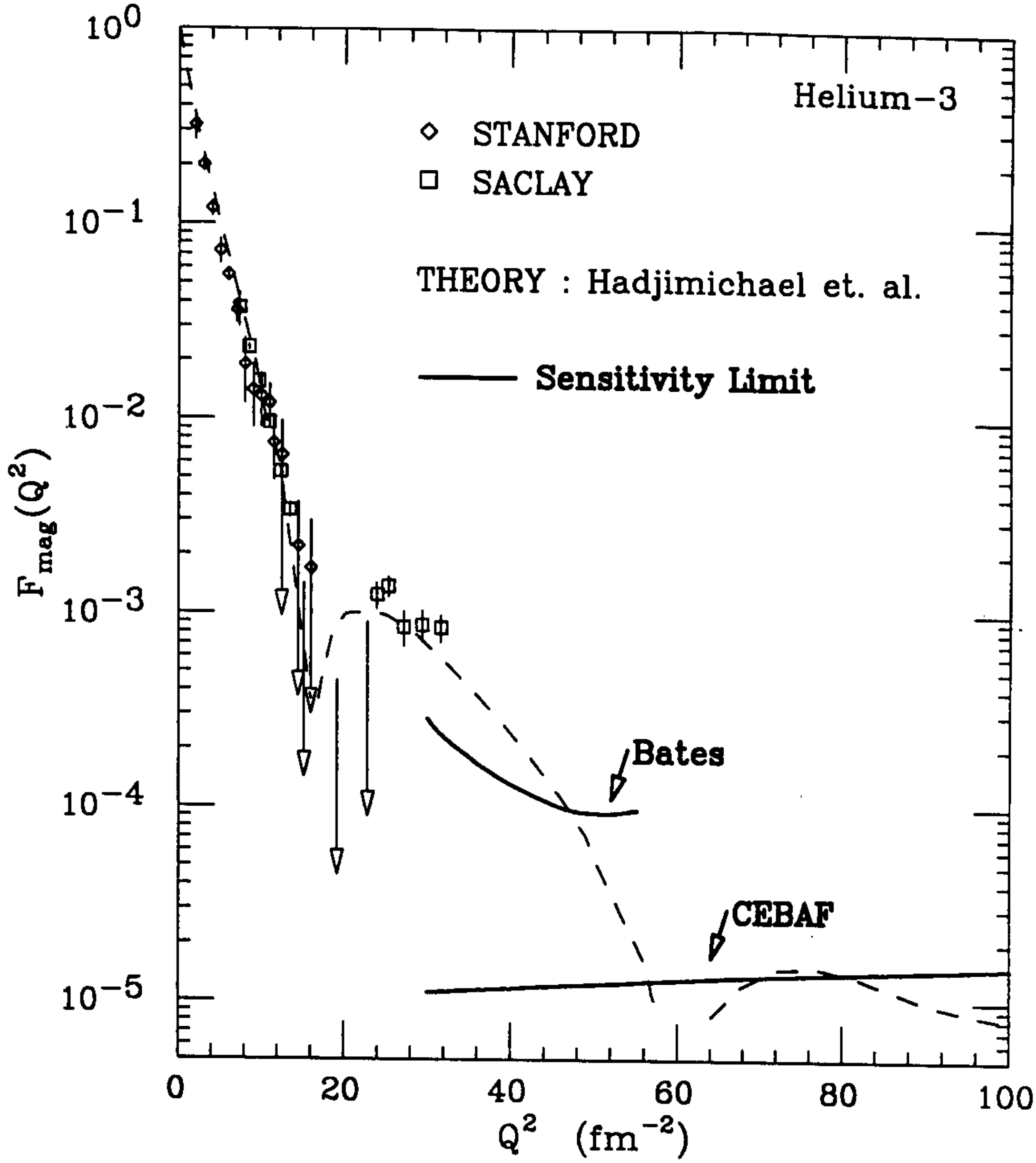
Helium−3
STANFORD
SACLAY
THEORY : Hadjimichael et. al.
Sensitivity Limit
Bates
CEBAF
$F_{mag}(Q^2)$
Q^2 (fm^{-2})
10^0
10^{-1}
10^{-2}
10^{-3}
10^{-4}
10^{-5}
0
20
40
60
80
100

Figure 1b

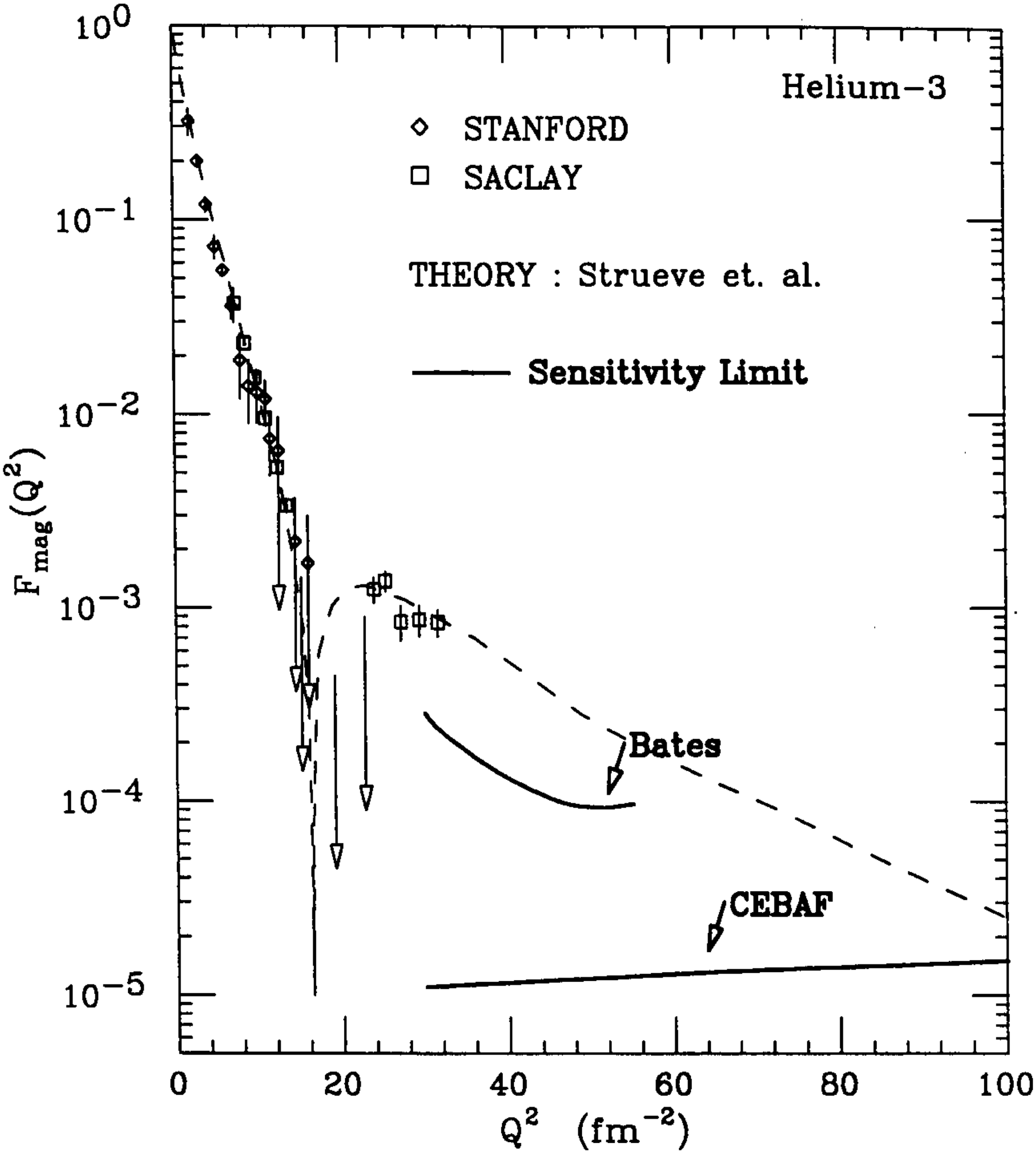
Helium-3
STANFORD
SACLAY
THEORY : Strueve et. al.
Sensitivity Limit
Bates
CEBAF
$F_{mag}(Q^2)$
Q^2 (fm^{-2})
10^0
10^{-1}
10^{-2}
10^{-3}
10^{-4}
10^{-5}
0
20
40
60
80
100

Figure 1c

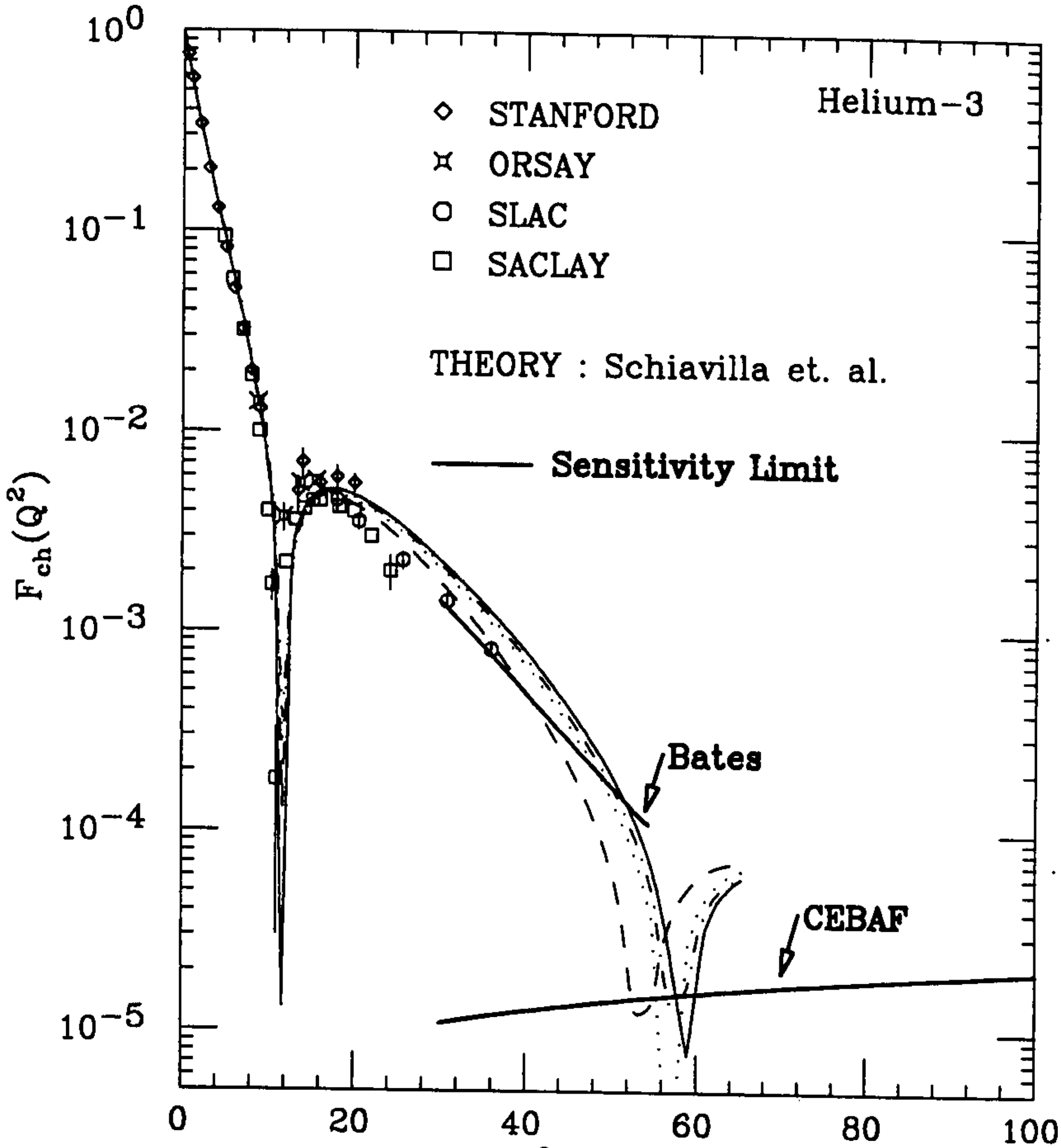

Helium-3
STANFORD
ORSAY
SLAC
SACLAY
THEORY : Schiavilla et. al.
Sensitivity Limit
Bates
CEBAF
$F_{ch}(Q^2)$
Q^2 (fm^{-2})
10^0
10^{-1}
10^{-2}
10^{-3}
10^{-4}
10^{-5}
0
20
40
60
80
100

Figure 2a

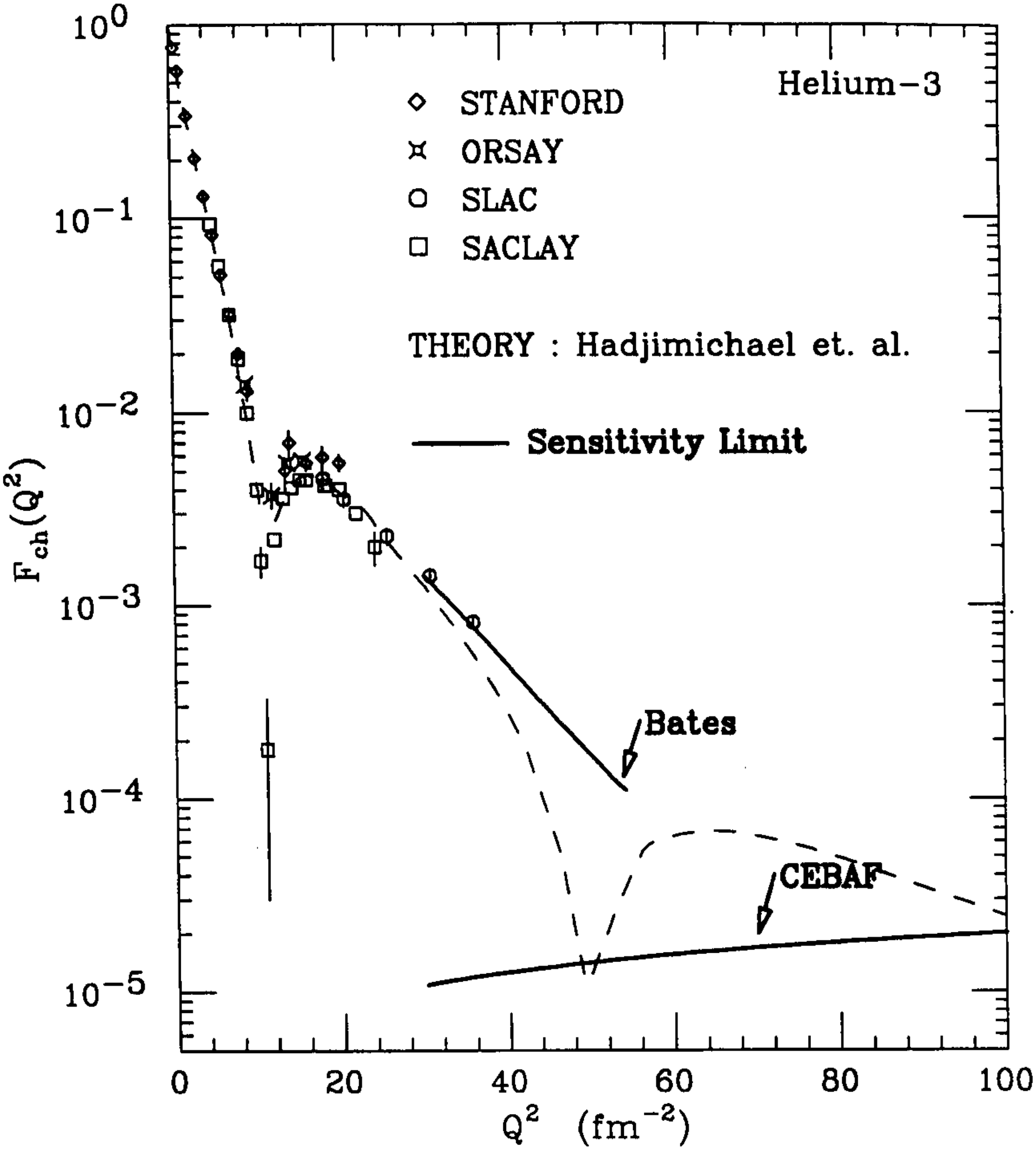

Helium-3
STANFORD
ORSAY
SLAC
SACLAY
THEORY : Hadjimichael et. al.
Sensitivity Limit
Bates
CEBAF
$F_{ch}(Q^2)$
Q^2 (fm^{-2})
10^0
10^{-1}
10^{-2}
10^{-3}
10^{-4}
10^{-5}
0
20
40
60
80
100

Figure 2b

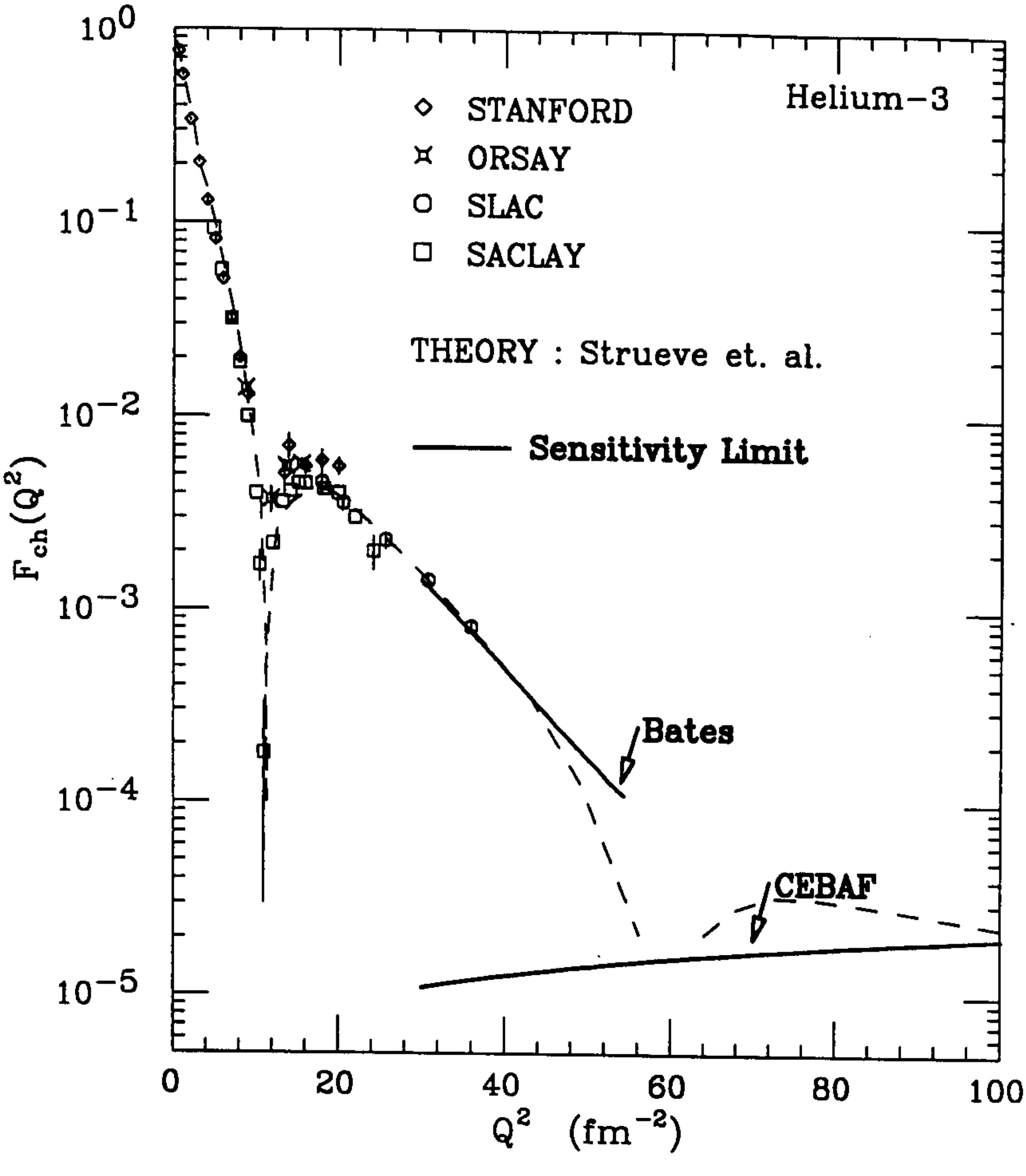

STANFORD
ORSAY
SLAC
SACLAY
Helium-3
THEORY : Strueve et. al.
Sensitivity Limit
Bates
CEBAF
10^0
10^{-1}
10^{-2}
10^{-3}
10^{-4}
10^{-5}
$F_{ch}(Q^2)$
0
20
40
60
80
100
Q^2 (fm^{-2})

Figure 2c